

New species of aquatic chytrids from Oman

Brandon T. Hassett , Badriya K. Al-Shaibi , Abdulrahman Al-Nabhani & Abdullah M. Al-Sadi

To cite this article: Brandon T. Hassett , Badriya K. Al-Shaibi , Abdulrahman Al-Nabhani & Abdullah M. Al-Sadi (2020) New species of aquatic chytrids from Oman, Mycologia, 112:4, 781-791, DOI: [10.1080/00275514.2020.1761226](https://doi.org/10.1080/00275514.2020.1761226)

To link to this article: <https://doi.org/10.1080/00275514.2020.1761226>



© 2020 The Author(s). Published with license by Taylor & Francis Group, LLC.



[View supplementary material](#)



Published online: 12 Jun 2020.



[Submit your article to this journal](#)



Article views: 195



[View related articles](#)



[View Crossmark data](#)

New species of aquatic chytrids from Oman

Brandon T. Hassett^a, Badriya K. Al-Shaibi^b, Abdulrahman Al-Nabhani^b, and Abdullah M. Al-Sadi^b

^aUiT–The Arctic University of Norway, Framstredet 6, Tromsø 9019, Norway; ^bDepartment of Crop Sciences, College of Agricultural and Marine Sciences, Sultan Qaboos University, P.O. Box-34, Al-Khod 123, Oman

ABSTRACT

Oman is a desert country in the south of the Middle East. Springs and other water sources that harbor aquatic organisms can be separated by hundreds of kilometers. In Oct 2019, we isolated four freshwater aquatic fungi (Chytridiomycota) from benthic detritus baited with pine pollen on a general nutrient medium near Salalah, Oman. Database queries of nuc 28S rRNA (28S) and internal transcribed spacer region ITS1-5.8S-ITS2 (ITS) revealed that one of these strains was *Dinocytrium kinnereticum*, a recently described algal pathogen from the Sea of Galilee. The other three strains had low molecular identity to available ITS sequences. These unknown strains varied in size and released endogenously swarming zoospores through papillae from mature zoosporangia. Zoospore ultrastructure was consistent with described species in the Rhizophydiales, and molecular phylogenetic results grouped these three strains into a clade in the genus *Rhizophyidium*. We circumscribe these three strains as a sp. nov., thereby expanding the diversity within *Rhizophyidium* described as the new species *R. jobii*. In doing so, we provide the first report of Chytridiomycota from Oman.

ARTICLE HISTORY

Received 29 January 2020
Accepted 23 April 2020

KEYWORDS

Chytridiomycota; Middle East; *Rhizophyidium*; zoospore; 1 new taxon

INTRODUCTION

Oman is situated in the southeast corner of the Arabian subcontinent. The Arabian subcontinent was last connected to Africa ~30 Ma, until the eventual formation of the Red Sea (Bohannon et al. 1989). To the north of Oman and Yemen is the Rub' Al Khali Desert (the Empty Quarter), which spans >600 000 square km of arid sand and dunes. The Arabian Sea sits to the south and east of Oman. As a result of its geographic position, the relative isolation of Oman renders it of potential interest for studies of allopatric speciation. Sporadic rainfall and perennial springs fill permanent and ephemeral water sources (wadis), further elevating interests in diversity driven by allopatric speciation, especially among freshwater aquatic organisms.


Oman has a relatively short history of fungal biology and ecology. To date, the majority of mycological research has been conducted within the realm of plant pathology (Al-Nadabi et al. 2018); consequently, the fungal species richness within Oman has historically been inferred from pathogen reports (Al-Bahry et al. 2005). In 2016, the first checklist of fungi in Oman was published (Maharachikumbura et al. 2016), coalescing all previous observations, while expanding that compilation with new observations, including the discovery of

novel taxa (Halo et al. 2019). However, there were no flagellated fungi in this checklist.

Chytridiomycota, primarily in the genus *Rhizophlyctis*, have been detected in high-throughput sequencing surveys throughout the Arabian Peninsula, including within Oman (Abed et al. 2013, 2019) and Saudi Arabia (Moussac et al. 2017). However, only three species of Chytridiomycota were reported between 1940 and 2016 from anywhere in the Middle East: *Synchytrium aureum* in Palestine, *Rhizophyidium racemosum* in Egypt (Mouchacca 2005, 2016), and *Dinocytrium kinnereticum* from the Sea of Galilee (Leshem et al. 2016). Despite a long history of Chytridiomycota studies in neighboring India (Karling 1964; Dayal 1997) and regular screenings for *Synchytrium* (Potato Export Guide 2019), to our knowledge, there have been no Chytridiomycota reported within Oman or on the Arabian Peninsula (Mouchacca 2005, 2016). As a result, the species richness of Chytridiomycota remains uncharacterized in this region.

To help fill this gap, we conducted a culturing survey within Oman. As a result of these efforts, we report four strains of Chytridiomycota, representing two different species. The first is the second report of *Dinocytrium kinnereticum* in the Chytridiales; the second, we describe as a novel species, *Rhizophyidium jobii* in the Rhizophydiales.

CONTACT Brandon T. Hassett  brandon.hassett@uit.no

 Supplemental data for this article can be accessed on the [publisher's website](#).

© 2020 The Author(s). Published with license by Taylor & Francis Group, LLC.

This is an Open Access article distributed under the terms of the Creative Commons Attribution License (<http://creativecommons.org/licenses/by/4.0/>), which permits unrestricted use, distribution, and reproduction in any medium, provided the original work is properly cited.

MATERIALS AND METHODS

Samples and cultures—Benthic detritus was collected from several freshwater springs and ephemeral standing water pools (<0.25 m depth) near Salalah, Oman (17.110°N, 53.995°E) on 10 Oct 2019. Samples were collected in sealable plastic bags and maintained at air temperature until processing (4 h from time of collection). A slurry of detritus and source water was incubated with heat-killed pine pollen at room temperature (~24 C) for 3 d. After 3 d, pollen was drop-streaked onto PmTG agar medium (peptonized milk, tryptone, glucose) containing streptomycin sulfate and penicillin G antibiotics (Barr 1986). After 24 h, individual Chytridiomycota zoosporangia were transferred to a separate PmTG plate to establish axenic cultures, where they were further maintained at room temperature until light microscopy examination and DNA extraction. Specimens were deposited in the Collection of Zoosporic Eufungi at the University of Michigan (CZEUM; czeum.herb.lsa.umich.edu/index.php).

Light microscopy—We incubated new subcultures 3 d prior to analysis and captured images of sporangia and zoospores with a Nikon H600L microscope fitted with a DS-Ri2 camera (Melville, New York). Cells were imaged directly on the agar plate to preserve their structural integrity while not introducing morphological artifacts. Ranges were reported by identifying the largest and smallest nonephemeral (minimum presence of three) cell stages.

DNA extraction, PCR, and sequencing—We extracted DNA from axenic cultures with a DNeasy PowerMax Soil Kit (Qiagen, Hilden, Germany), following the manufacturer's protocols. A portion of nuc 28S rDNA (28S) and the internal transcribed spacer region ITS1-5.8S-ITS (ITS) were amplified with primers ITS4/ITS5 (White et al. 1990) and LR0R/LR5 (Vilgalys and Hester 1990; Cubeta et al. 1991) in Illustra PuReTaq Ready-To-Go PCR Beads (GE Healthcare, Pittsburgh, Pennsylvania). Amplicon purification and Sanger sequencing were conducted commercially by Macrogen (Seoul, Korea). Samples were sequenced bidirectionally to maximize confidence in automated base calls along the length of the amplicon. Sequence results (.AB1 files) were analyzed in MEGA 7.0.26 (Kumar et al. 2016) and explored for the presence of ambiguous peaks and poor-quality reads.

Phylogenetic analysis—Nucleotide queries were conducted in GenBank. From these queries, two nucleotide data

sets were compiled: the first for Chytridiales and the second for Rhizophydiales. For OAS2, 5, and 6, which allied to the order Rhizophydiales, multiple sequence alignments (MSAs) were created using type strains from this order, additional strains of *Rhizophyidium*, and outgroup strains in the Rhizophlyctidales and Spizellomycetales (TABLE 1). Specifically, we aligned ITS and 28S loci separately using the online version of MAFFT 7 (Katoh et al. 2002, 2017). MSAs were visually inspected and manually edited in AliView 1.26 (Larsson 2014; by end-trimming sequences to equal length, removing insertions that existed in a single sequence, and manually correcting nucleotide misalignments). Loci were concatenated in SeaView 4.6.1 (Gouy et al. 2010). The concatenated alignment was partitioned by locus, as determined by the “greedy” algorithm (Lanfear et al. 2012) of PartitionFinder 2.1.1 (Lanfear et al. 2016). A maximum likelihood (ML) phylogeny was inferred with a GTR+G model of evolution, identified as the best substitution model in PartitionFinder. Bootstrap values were generated from 1000 pseudoreplicates on the concatenated ITS-28S MSA in RAxML 8.0.0 (Stamatakis 2006, 2014; Stamatakis et al. 2008). To supplement ML inferences, Bayesian inference (BI) analysis was conducted with MrBayes 3.2.7a (Ronquist et al. 2012) using the GTR+G model with 10 million generations (typically a sufficient number of generations for the standard deviation of split frequencies to fall below 0.01), sampling trees every 100 generations and applying a 25% burn-in to calculate posterior probabilities (PPs).

For OAS3, which was allied to the taxonomic order Chytridiales, the alignment of Leshem et al. (2016) was downloaded from TreeBASE (S17951), expanded with 28S sequence of this strain, and subsequently aligned using MAFFT, and manually edited in AliView as described above. A ML phylogeny was inferred with the GTR+G model of evolution (identified as best substitution model with PartitionFinder) and subsequently bootstrapped after 1000 pseudoreplications in RAxML. Trees and alignments for Chytridiales and Rhizophydiales used in this analysis were deposited in TreeBASE (S26062).

Transmission electron microscopy—Several agar plates of Chytridiomycota strain OAS6 were grown at room temperature for 3 d. Zoospores were harvested by first flooding plates with sterile water and waiting for zoospore release (Letcher and Powell 2005). Once sufficient zoospores were present, they were harvested by pipette and transferred to a 1.5-mL microcentrifuge tube. Zoospores were fixed in a solution of 2.5% glutaraldehyde in 0.1 M sodium cacodylate buffer (pH 7.4) for 2 h at 22 C, followed by an additional 20 h at 4 C. Fixed zoospores

Table 1. NCBI accession numbers for isolated Omani Chytridiomycota.

Isolate	ITS	28S
<i>Alphamyces chaetifer</i> ARG025	NR_119646	NG_060383
<i>Angulomyces argentinensis</i> ARG008	NR_119644	NG_042447
<i>Aquamyces chlorogonii</i> ARG018	NR_119645	EF585603
<i>Boothomyces macroporosum</i> PL-AUS-21	NR_119591	AY439040
<i>Borealophlyctis paxensis</i> BR368	—	NG_042455
<i>Borealophlyctis nickersoniae</i> WJD170	—	KR349612
<i>Collimyces mutans</i>	LC274663	LC274662
<i>Coralloidiomyces digitatus</i> PL163L	NR_119652	NR_042452
<i>Dinomyces arenysensis</i> P234	KJ027542	KJ027539
<i>Fimicolochytrium alabamae</i> JEL538	—	NG_060390
<i>Globomyces pollinis-pini</i> ARG068	NR_119649	NG_042451
<i>Gorgonomycetes haynaldii</i> ARG026	NG_042448	NG_042448.1
<i>Halomyces littoreus</i> Barr263	DQ485604	DQ485540
<i>Kappamyces laurelensis</i> _PL98	—	AY439034
OAS2 (Rhizophydiales)	MN787065	MN759467
OAS3 (<i>Dinochytrium kinnereticum</i>)	MN787068	MN759468
OAS5 (Rhizophydiales)	MN787066	MN759469
OAS6 (Rhizophydiales)	MN787067	MN759470
<i>Operculomyces laminatus</i> JEL223	NR_119590	NG_042440
<i>Paludomyces mangrovei</i> ATCC26191	NR_138404	NG_059549
<i>Paranomyces uniporus</i> PL157	DQ485685	DQ485594
<i>Pateramyces corrientinensis</i> ARG046	NR_111261	NG_042449
<i>Protrudomyces lateralis</i> ARG071	NR_119650	NG_060073
<i>Rhizophlyctis rosea</i> WJD106	—	KR349614
<i>Rhizophlyctis rosea</i> WJD197	—	KR349615
<i>Rhizophyidium globosum</i> JEL222	—	DQ485551
<i>Rhizophyidium</i> sp. ARG013	EF585638	EF585598
<i>Rhizophyidium</i> sp. ARG014	EF585639	EF585599
<i>Rhizophyidium</i> sp. ARG016	EF585641	EF585601
<i>Rhizophyidium</i> sp. ARG035	EF585653	EF585613
<i>Rhizophyidium</i> sp. ARG051	EF585660	EF585620
<i>Rhizophyidium</i> sp. ARG052	EF585661	EF585621
<i>Rhizophyidium</i> sp. ARG055	EF585662	EF585622
<i>Rhizophyidium</i> sp. Barr107	DQ485602	DQ485538
<i>Rhizophyidium</i> sp. JEL136	—	AY349086
<i>Rhizophyidium</i> sp. JEL292	DQ485620	DQ485554
<i>Rhizophyidium</i> sp. JEL294	DQ485621	DQ485555
<i>Rhizophyidium</i> sp. MP043	—	KC691334
<i>Rhizophyidium</i> sp. MP049	—	KC691336
<i>Rhizophyidium</i> sp. MP050	—	KC691337
<i>Rhizophyidium</i> sp. PL149A	DQ485682	DQ485591
<i>Rhizophyidium</i> sp. PL-AUS Ad014	DQ485647	DQ485570
<i>Rhizophyidium</i> sp. PL-AUS-R002	DQ485648	DQ485571
<i>Rhizophyidium</i> sp. WJD145	—	KC691393
<i>Rhizophyidium</i> sp. MP042	—	KC691333
<i>Rhizophyidium echinocystoides</i> B8	—	MH933969
<i>Staurastromyces oculus</i> STAU-CHY3	KY350146	KY350145
<i>Terramyces subangulosum</i> PL003	NR_119592	DQ485582
<i>Tripartalcar eqii</i> WJD156	—	NG_059952
<i>Uebelmesseromyces harderi</i> ATCC24053	DQ485595	AY349087
<i>Urceomyces sphaerocarpus</i> ARG048	NR_119648	NG_042450
OAS2 (Rhizophydiales)	MN787065	MN759467
OAS3 (<i>Dinochytrium kinnereticum</i>)	MN787068	MN759468
OAS5 (Rhizophydiales)	MN787066	MN759469
OAS6 (Rhizophydiales)	MN787067	MN759470
<i>Rhizophyidium</i> sp. JEL136	—	AY349086
<i>Rhizophyidium</i> sp. Barr107	DQ485602	DQ485538
<i>Rhizophyidium globosum</i> JEL222	—	DQ485551
<i>Rhizophyidium</i> sp. JEL294	DQ485621	DQ485555
<i>Rhizophyidium</i> sp. JEL292	DQ485620	DQ485554
<i>Rhizophyidium</i> sp. MP049	—	KC691336
<i>Rhizophyidium</i> sp. PL-AUS-R002	DQ485648	DQ485571
<i>Rhizophyidium</i> sp. ARG013	EF585638	EF585598
<i>Rhizophyidium</i> sp. ARG014	EF585639	EF585599
<i>Rhizophyidium</i> sp. MP042	—	KC691333
<i>Rhizophyidium</i> sp. ARG035	EF585653	EF585613
<i>Rhizophyidium</i> sp. ARG016	EF585641	EF585601
<i>Rhizophyidium</i> sp. MP043	—	KC691334
<i>Rhizophyidium</i> sp. PL149A	DQ485682	DQ485591
<i>Rhizophyidium</i> sp. ARG051	EF585660	EF585620
<i>Rhizophyidium</i> sp. ARG052	EF585661	EF585621
<i>Rhizophyidium</i> sp. ARG055	EF585662	EF585622

(Continued)

Table 1. (Continued).

Isolate	ITS	28S
<i>Rhizophyidium</i> sp. WJD145	—	KC691393
<i>Rhizophyidium</i> sp. PL-AUS Ad014	DQ485647	DQ485570
<i>Rhizophyidium</i> sp. MP050	—	KC691337
<i>Staurastromyces oculus</i> STAU-CHY3	KY350146	KY350145
<i>Uebelmesseromyces harderi</i> ATCC24053	DQ485595	AY349087
<i>Boothiomycetes macroporosum</i> PL-AUS-21	NR_119591	AY439040
<i>Terramyces subangulosum</i> PL003	NR_119592	DQ485582
<i>Angulomyces argentinensis</i> ARG008	NR_119644	NG_042447
<i>Aquamyces chlorogonii</i> ARG018	NR_119645	EF585603
<i>Protrudomyces lateralis</i> ARG071	NR_119650	NG_060073
<i>Rhizophyidium echinocystoides</i> B8	—	MH933969
<i>Collimyces mutans</i>	LC274663	LC274662
<i>Coralloidiomyces digitatus</i> PL163L	NR_119652	NG_042452
<i>Dinomyces arenysensis</i> P234	KJ027542	KJ027539
<i>Pateramyces corrientinensis</i> ARG046	NR_111261	NG_042449
<i>Urceomyces sphaerocarpus</i> ARG048	NR_119648	NG_042450
<i>Globomyces pollinis-pini</i> ARG068	NR_119649	NG_042451
<i>Alphamyces chaetifer</i> ARG025	NR_119646	NG_060383
<i>Operculomyces laminatus</i> JEL223	NR_119590	NG_042440
<i>Halomyces littoreus</i> Barr263	DQ485604	DQ485540
<i>Paludomyces mangrovei</i> ATCC26191	NR_138404	NG_059549
<i>Paranomyces uniporus</i> PL157	DQ485685	DQ485594
<i>Kappamyces laurelensis</i> PL98	—	AY439034
<i>Tripalticalcar eqii</i> WJD156	—	NG_059952
<i>Fimicolochytrium alabamae</i> JEL538	—	NG_060390
<i>Borealphlyctis paxensis</i> BR368	—	NG_042455
<i>Borealphlyctis nickersoniae</i> WJD170	—	KR349612
<i>Rhizophlyctis rosea</i> WJD197	—	KR349615
<i>Rhizophlyctis rosea</i> WJD106	—	KR349614
<i>Gorgonomycetes haynaldii</i> ARG026	NG_042448	NG_042448.1

were pelleted by centrifugation at 1000 rpm for 20 min. The pelleted zoospores were washed two times in 0.1 M sodium cacodylate buffer (pH 7.4) and postfixed in 1% osmium tetroxide for 1 h at 22 C. The pellet was washed twice with distilled water and embedded in HistoGel (Richard-Allan Scientific, San Diego, California). The solidified HistoGel containing zoospores was dissected into 1-mm³ pieces and dehydrated in a graded series (25%, 75%, and 95%) of acetone for 10 min per step. After this graded series, the HistoGel block was rinsed twice in 100% acetone for 20 min. The blocks were then embedded in araldite cy212 epoxy resin and polymerized for 20 h at 60 C. Sections were cut with a diamond knife using a Reichert Ultracut E microtome (Leica, Wetzlar, Germany) and oriented on a copper grid. Sections were poststained for 20 min using uranyl acetate followed by lead citrate for 15 min. Stained sections were examined with a JEM-2100 field emission electron microscope (JEOL, Tokyo, Japan).

RESULTS

Several locations containing standing freshwater were sampled from the Salalah region in southern Oman and subsequently baited with pine pollen. From these efforts, Chytridiomycota were cultivated at only one location. After nucleotide extraction, amplification, and sequencing, GenBank queries revealed that from among these strains, OAS2, 5, and 6 had highest identity (83% ITS) to

Rhizophyidium sp. PL-AUS-Ad014 (DQ485647) and (95% 28S) to *Rhizophyidium* sp. ARG016 (EF585601). These three strains had 1 bp difference over the length of our 28S fragment and 3 bp differences across the ITS. By contrast, OAS3 had highest sequence identity (93% ITS) to *Chytridium lagenaria* (FJ822972) and (100% 28S) to *Dinocytrium kinnereticum* (KT281910).

Light microscopy—On PmTG agar, strains OAS2, 5, and 6 produced oval to spherical 2.5–5.5 µm diam zoospores that developed into oval to spherical germlings (FIG. 1A). Germlings possessed a single rhizoidal axis that basally extended 5–15 µm in length before terminally branching into secondary and tertiary rhizoids (FIG. 1B, C). In near-mature and mature zoosporangia, this rhizoidal axis could expand to form a thick central rhizoidal axis (~5 µm wide) that would support the zoosporangium (FIG. 1D, E, F). Mature zoosporangia varied in size (20–150 µm diam) and variably possessed 1–5 prominent papillae (FIG. 1G, H, I). Before discharge, zoospores became motile within the sporangium. Zoosporangia were observed releasing zoospores sequentially through upraised pores (FIG. 1J), resulting in collapsed zoosporangia (FIG. 1K, L).

On PmTG agar medium, the strain with 100% 28S identity to *D. kinnereticum* released elongated zoospores through an operculum, could parasitize itself, and

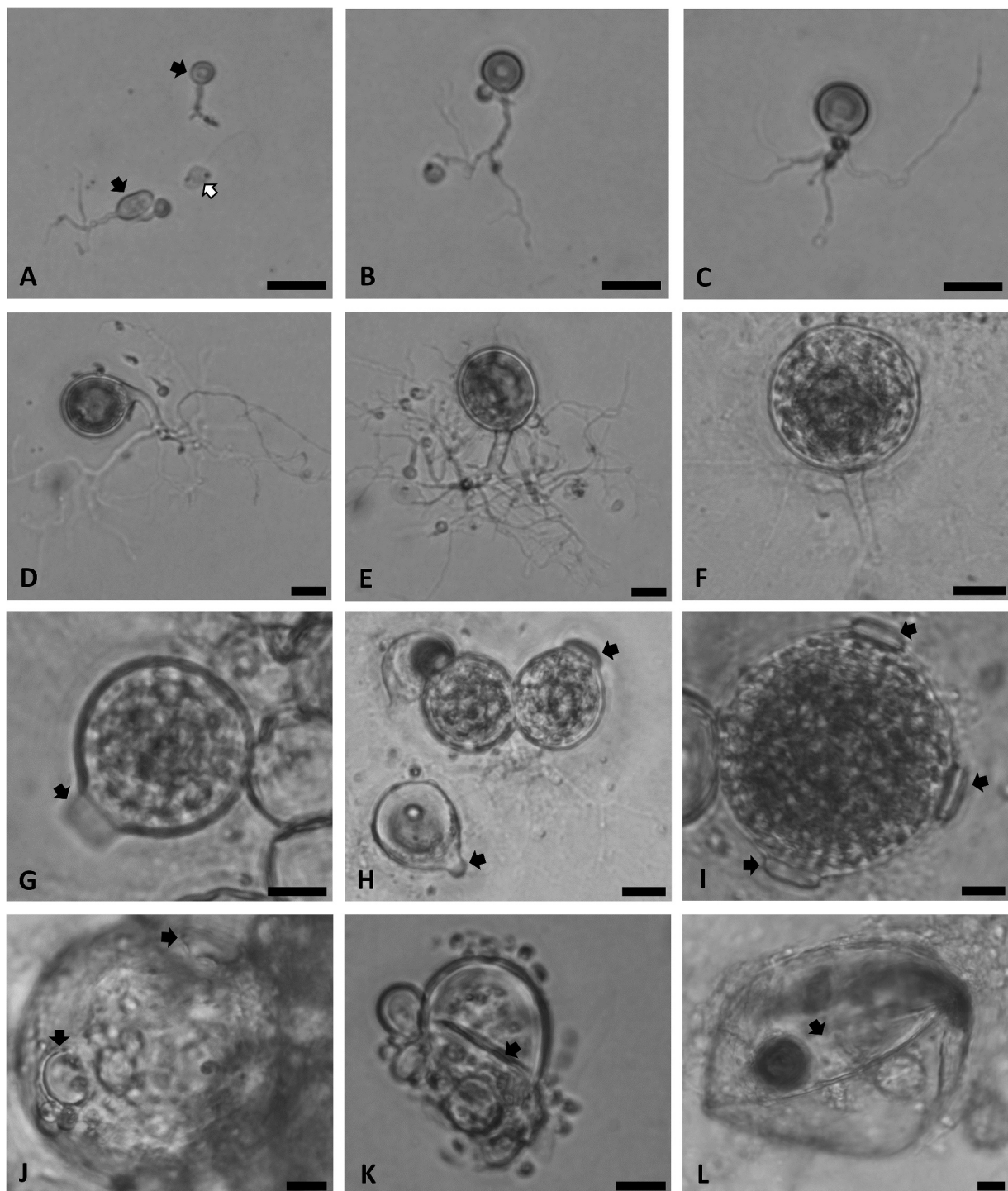


Figure 1. *Rhizophydium jobii* (OAS6; holotype). A. Germlings (black arrows) adjacent to a zoospore (white arrow). Bottom left germling is self-parasitized. B. Developing germling with a well-defined single rhizoidal axis terminally branching. C. Immature zoosporangia with basal rhizoids. D–F. Zoosporangium supported by prominent stalk that branches into rhizoids. G–I. Papillated (black arrows) zoosporangia with 1–3 discharge papillae. J. Zoosporangium with pores through which zoospores escape (black arrows). K–L. Collapsed zoosporangium (black arrows) after zoospore release. Bars = 10 μm .

possessed swellings basal to a developing zoosporangium that could mature into a prominent apophysis (FIG. 2).

Zoospore ultrastructure—Of the three strains molecularly allied to *Rhizophydium*, strain OAS6 was selected for transmission electron microscopy (TEM). The zoospores

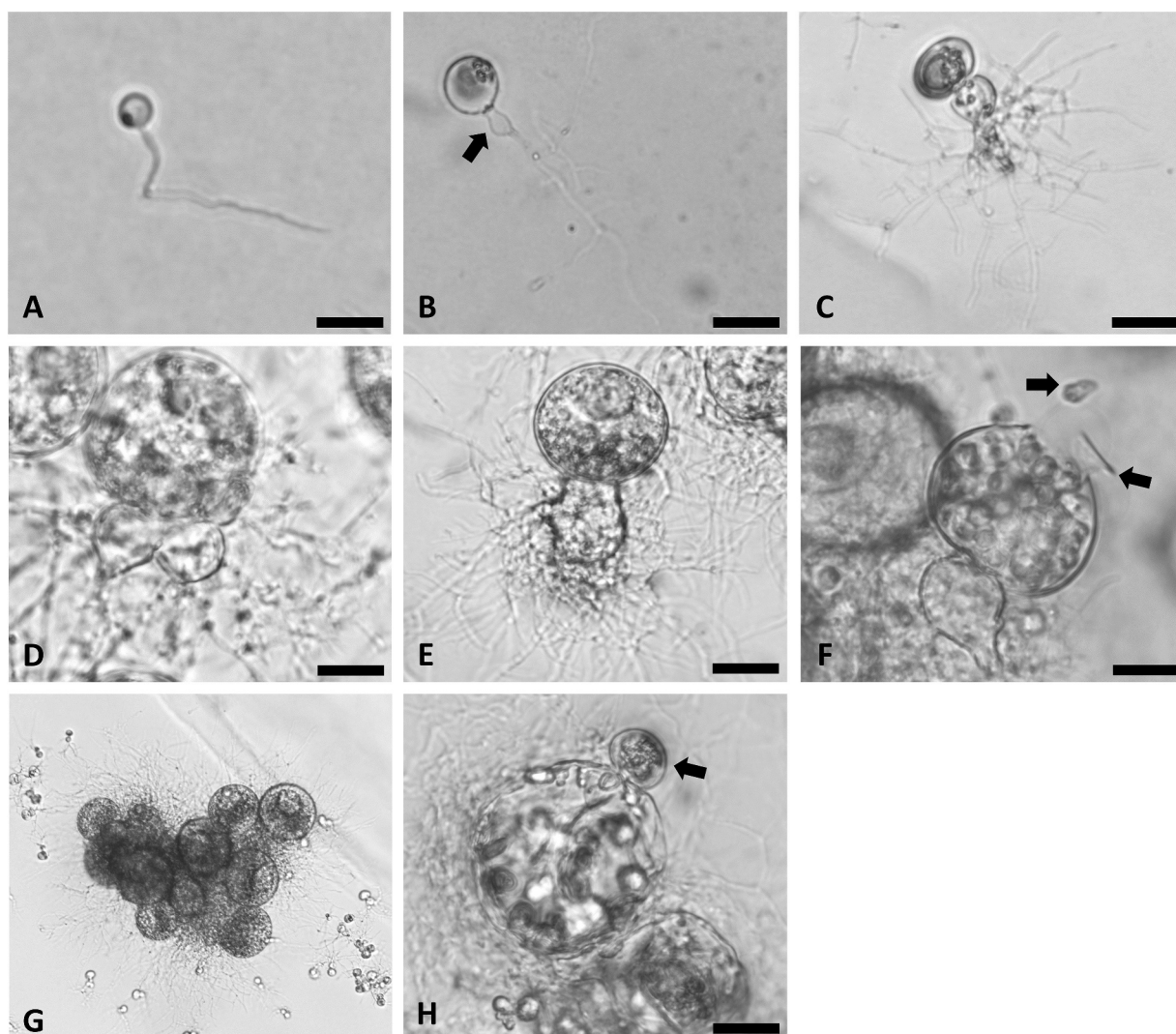


Figure 2. *Dinochytrium kinnereticum* (OAS3). A. Germling with a single rhizoidal axis. B. Developing germling with small rhizoids branching from a prominent rhizoidal axis. Developing apophysis (arrow) basal to an immature zoosporangium. C. Immature zoosporangium with extensively branched rhizoids basal to an apophysis. D–E. Mature zoosporangia with well-developed apophyses (infrequently two, D) and extensively branched rhizoids. F. Zoospore (upper arrow) escaping from an operculum in the cell wall (lower arrow). G. Large cluster of zoosporangia, each with a diam >100 µm surrounded by more typical smaller, mature zoosporangia. H. Empty zoosporangia with an immature sporangium developing on surface of empty zoosporangium (arrow). Bars = 10 µm.

were similar to those of members of Rhizophydiales (Letcher et al. 2008) in that they possessed a ribosomal aggregation surrounded by endoplasmic reticulum (FIG. 3A, B, D), and external to the ribosomal aggregation, a lipid globule with an adnate rumposome (FIG. 3C) and microbody (FIG. 3E), mitochondria (FIG. 3A, D), and nucleus (FIG. 3A, B). Zoospores lacked a dense area in the transition area of the flagellum (FIG. 3A, B, D, E, F). A hemispherical vesicular area was present between the kinetosome and the ribosomal aggregation (FIG. 3D, F). The kinetosome and nonflagellated centriole were nearly parallel and connected by moderately electron-dense fibrillar material in a broad zone of convergence (FIG. 3F). After exploring hundreds of sections, OAS6 zoospores appeared to lack a spur over the kinetosome,

a microtubule root from the kinetosome to the rumposome, and an electron-dense flagellar plug. Electron-dense inclusions were consistently present near the base of the flagellum.

Molecular phylogeny—The ML phylogeny of the Rhizophydiales placed strains OAS2, 5, and 6 in the genus *Rhizophyidium* with strong support (FIG. 4). These three strains were monophyletic with 100% bootstrap support, whereas *Pateramyces corrientinensis* and *Staurastromyces oculus* grouped sister to *Rhizophyidium* with 76% ML bootstrap support. Within *Rhizophyidium*, OAS strains grouped sister to the morphologically uncharacterized strain MP049, but with poor ML

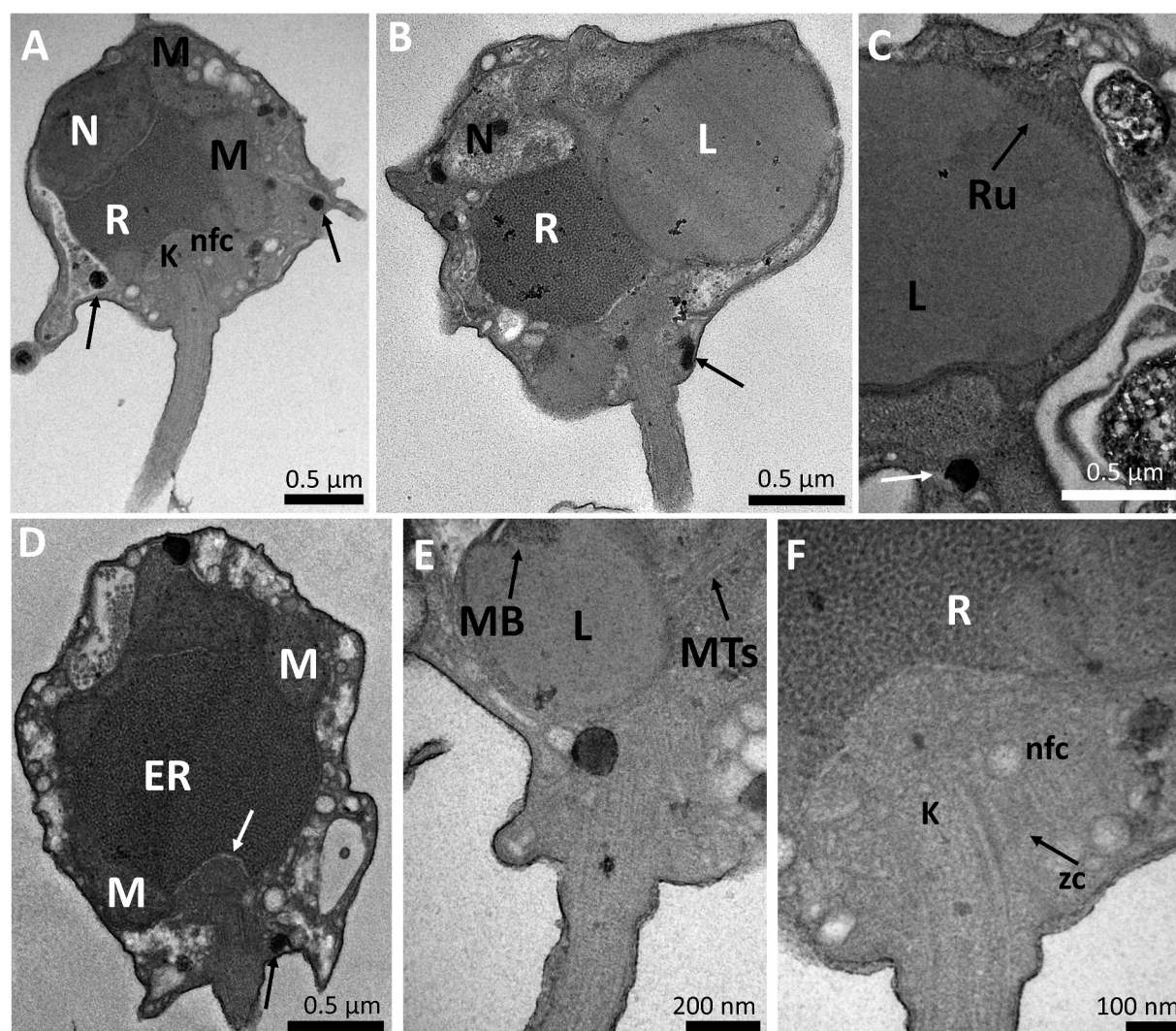


Figure 3. *Rhizophydium jobii* (OAS6). A. Zoospore longitudinal sections with nucleus (N), mitochondria (M), ribosomal aggregation (R), kinetosome (K), nonflagellated centriole (nfc), and dark inclusions (arrow). B. Zoospore longitudinal section showing a nucleus adjacent to the ribosomal aggregate, which is adjacent to a lipid (L). C. Lipid with fenestrated rumposome (Ru). D. Central ribosomal aggregate with dark endoplasmic reticulum (ER). At base of aggregate a hemispherical vesicular area (white arrow). E. Lipid inclusion with microbody (MB) with what appears to be microtubules (MTs). F. Magnified section of part A. Nonflagellated centriole parallel to kinetosome, basal to ribosomal aggregation, with broad zone of convergence (zc) between kinetosome and nonflagellated centriole (arrow).

support. BI analysis of the Rhizophydiales produced an identical topology to that by ML inferences, with greater than or equal support for all nodes. In the ML phylogeny of combined ITS-28S of *Rhizophydium*, the OAS strains grouped with 100% bootstrap support, yet branched sister to a clade containing other uncharacterized strains, MP043 and ARG016, also with poor support (SUPPLEMENTARY FIG. 1).

Tests of phylogenetic hypotheses with ML analysis of the expanded alignment from Lesham et al. (2016) placed OAS3 in *Dinochytrium kinnereticum* with 100% bootstrap support (SUPPLEMENTARY FIG. 2).

TAXONOMY

Rhizophydium jobii Hassett, sp. nov. FIG. 1F

Mycobank MB835161

Typification: OMAN. SALALAH: Near tomb of Job (17.110°N, 53.995°E), from benthic detritus baited with pine pollen, 10 Oct 2019, B.T. Hassett OAS6 (**holotype**; FIG. 1F). Ex-type culture OAS6 (CZEUM). GenBank: ITS = MN787067; 28S=MN759470.

Etymology: *jobii* (Latin), named after Job (Ayyüb), an important figure throughout the Abrahamic religions, whose purported Omani tomb is near the collection site of these strains.

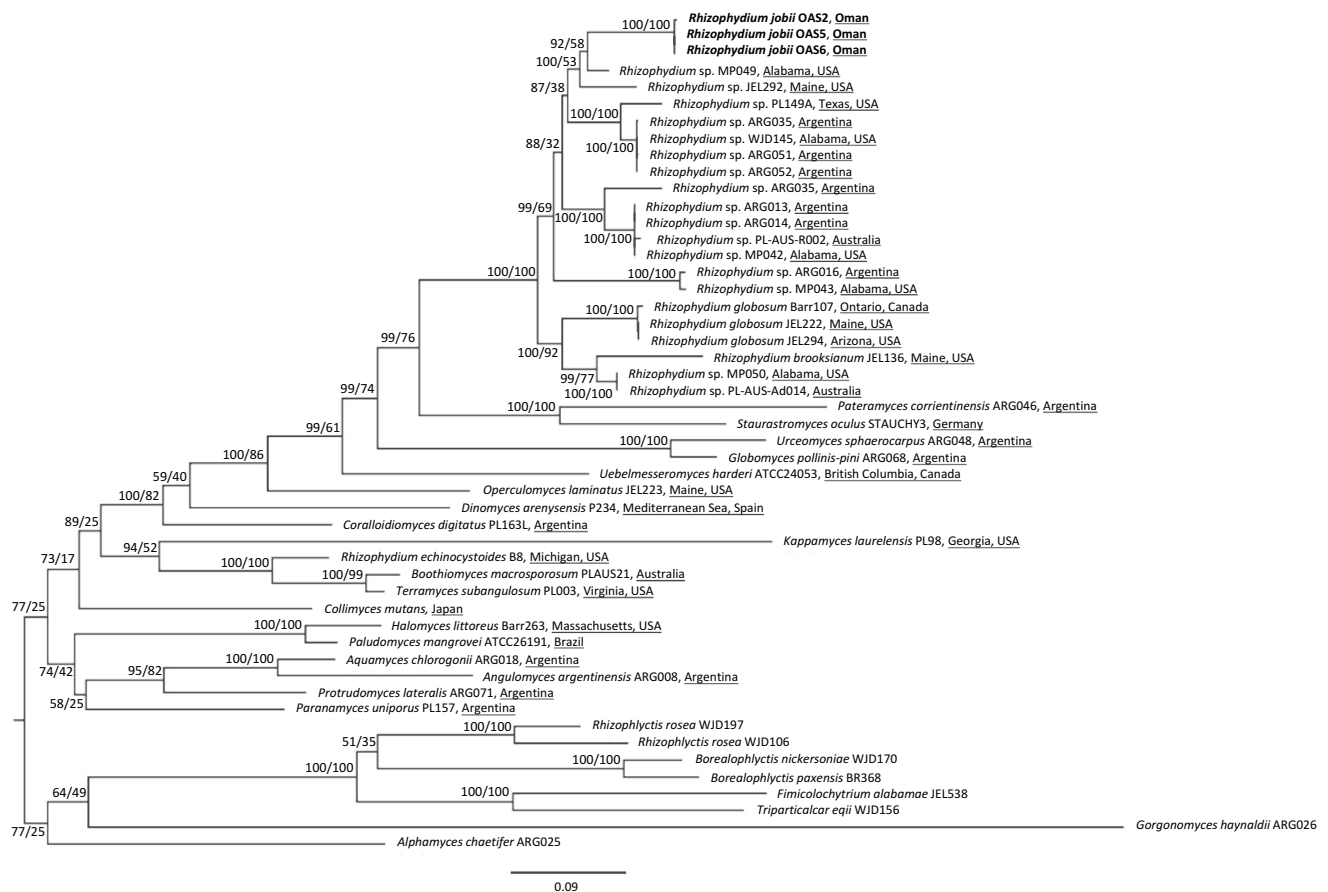


Figure 4. ML tree of Rhizophydiales inferred from analysis of combined ITS and 28S data. Nodes labeled with values (PP/ML bootstrap proportions). The new species, *Rhizophyidium jobii*, is indicated in bold. Members of the Rhizophlyctidales and Spizellomycetales were used as outgroups.

Diagnosis: Distinguished from *Rhizophyidium globosum* and *R. brooksianum* by the absence of a prominent laminated spur in TEM analysis of zoospores and by phylogenetic inference.

Description: Thallus monocentric, eucarpic, sporangium epibiotic, inoperculate. Mature zoosporangia variable in size (20–150 µm diam) and inconsistently possess 1–5 papillae. Prior to discharge, zoospores motile within zoosporangium. Zoospores released sequentially through apical pores in the cell wall. Zoospores oval to spherical, 2.5–5.5 µm diam, form a singular rhizoidal axis that terminally furcates and can thicken to support a mature zoosporangium. Zoospores posteriorly uniflagellate, contain lipid-associated microbody and rumposome; kinetosome and nonflagellated centriole nearly parallel with broad zone of convergence; aggregate of electron-dense vesicles in the posterior of the zoospore. Resting spore not observed.

Other specimen examined: OMAN. SALALAH: Same as type locality, from benthic detritus baited with pine pollen, 10 Oct 2019, *B.T. Hassett* OAS2, OAS5 (CZEUM).

DISCUSSION

From a single sample in Oman, *Dinocytrium kinnereticum* was recovered from benthic detritus in an ephemeral freshwater pool. The reisolation of *D. kinnereticum* in Oman is not surprising, as it was originally isolated from the Sea of Galilee (Leshem et al. 2016) within the greater Middle East region. Regardless, the reisolation of *Dinocytrium kinnereticum* in Oman expands the geographic range of this species and suggests that *D. kinnereticum* is likely widely distributed, aided by nutritional mode plasticity, inferred by its reported facultative parasitism of dinoflagellates. In general, the host range of Chytridiomycota is increasingly difficult to discern due in part to their ability to aerially disperse (Tipton et al. 2019). Consequently, any perceived biogeography could be driven by sampling effort.

Our other three strains, with nearly identical ITS sequences, formed a species-level clade within the taxonomic order Rhizophydiales. The resulting trees were congruent with other taxonomic studies of the Rhizophydiales (Van den Wyngaert et al. 2017). The

Omani strains clustered within *Rhizophydium*; however, in the expanded Rhizophydiales tree (FIG. 4), OAS strains group sister to MP049, whereas in the *Rhizophydium* tree (SUPPLEMENTARY FIG. 1) they group sister to MP043. In both trees, there was low support for deeper branches within *Rhizophydium*, underscoring the need for expanded sampling efforts to resolve ambiguous phylogenetic relationships among the geographically diverse strains circumscribed within this genus (Letcher et al. 2006, 2008; Davis et al. 2013).

Many previously described Chytridiomycota taxa are awaiting rediscovery and subsequent assignment of nucleotide information. The majority of *Rhizophydium* species are morphologically defined, missing type material, and lack molecular annotation (Letcher and Powell 2012). Morphologically, the size range and presence of an exit orifice observed in *R. jobii* is consistent with *Rhizophydium polystomum* from New Zealand (Karling 1968), which is among the many species without available sequence data. Although morphologically similar, *R. jobii* has prominent exit papillae, contrary to Karling's description of *R. polystomum* that it possesses "barely perceptible" exit papillae. In addition, *R. jobii* is morphologically congruent with a vague description of *R. signyense* (Willoughby 1971), originally isolated from soil in Antarctica and described as "saprophytic on chitin." This species, also without sequence data, has branched rhizoids attached at a single point and papillae that deliquesce to liberate zoospores. The morphological congruence of *R. jobii* with the description assigned to *R. signyense* hinders the ability to definitively exclude the possibility of *R. signyense* re-isolation. However, the great distance between Oman and Antarctica, as well as *R. jobii*'s ability to grow in the absence of chitin, renders it unlikely to be the same organism described by Willoughby.

Overall, the ultrastructural characteristics of *R. jobii* are congruent with many described species within the Rhizophydiales. Specifically, *R. jobii* had a hemispherical vesicular area between the kinetosome and the ribosomal aggregation, possessed numerous electron-dense inclusions dispersed throughout the zoospore, and lacked a flagellar plug, consistent with other descriptions of strains within Rhizophydiales. Although morphologically congruent with the Rhizophydiales and molecularly allied to *Rhizophydium*, *R. jobii* possessed unique zoospore ultrastructural features that are incongruent with *Rhizophydiaceae* and the sole genus it circumscribes, *Rhizophydium*. Specifically, both family and genus are characterized as having zoospores with (i) a laminated curved spur present, (ii) a kinetosome and nonflagellated centriole connection with a wide zone of convergence, and (iii) a microtubule root present

(Letcher et al. 2006, 2008). Based on TEM analysis, our strain is similar by possessing a wide zone of convergence between the kinetosome and the nonflagellated centriole; however, it is unique by possessing electron-dense vesicles in the posterior of the zoospore, while missing a laminated curved spur and a microtubule root. These unique ultrastructural features support previous hypotheses that *Rhizophydiaceae* could contain multiple genera (Letcher et al. 2008). As many strains molecularly allied to *Rhizophydium* remain morphologically uncharacterized, we chose to neither emend the family and genus descriptions nor erect a monotypic genus. If additional *Rhizophydium* species are found to possess similar ultrastructural features to *R. jobii*, it would seem appropriate to establish a separate genus.

Ultimately, we believe that these OAS strains represent a new species due to low percent identity to other *Rhizophydium* sp. strains, low bootstrap support for inclusion of other strains in the species, long branch lengths between *R. jobii* and other strains, and the unique morphological features of the zoospore. Although relationships within the genus *Rhizophydium* remain unresolved, these strains expand the known range of Chytridiomycota onto the Arabian Peninsula, while expanding the diversity within the Rhizophydiales.

ACKNOWLEDGMENTS

William Davis completed the ML phylogenetic analysis for the manuscript and provided interpretation, and we thank him for this major contribution. We thank the executive editor, P. B. Matheny, and associate editor, J. Stajich, for edits and suggestions that improved earlier versions of the manuscript.

Funding

Brandon T. Hassett is supported by the United States Fulbright Scholar program, as part of the "Illustrated Field Guide to Fungi of Oman" project. The authors thank Sultan Qaboos University for partial support of the study.

ORCID

Brandon T. Hassett  <http://orcid.org/0000-0002-1715-3770>
Abdullah M. Al-Sadi  <http://orcid.org/0000-0002-3419-8268>

LITERATURE CITED

Abed RMM, Al-Sadi AM, Al-Shehi M, Al-Hinai S, Robinson MD. 2013. Diversity of free-living and lichenized communities in biological soil crusts of the Sultanate of Oman and their role in improving soil properties. *Soil Biology and Biochemistry* 57:695–705.

- Abed RMM, Tamm A, Hassenrück C, Al-Rawahi AN, Rodríguez-Caballero E, Fiedler S, Maier S, Weber B. 2019. Habitat-dependent composition of bacterial and fungal communities in biological soil crusts from Oman. *Scientific Reports* 9:6468.
- Al-Bahry S, Elshafie AE, Deadman M, Al Sa'di A, Al Raesi A, Al Maqbali Y. 2005. First report of *Ganoderma colossus* on *Ficus altissima* and *Delonix regia* in Oman. *Plant Pathology* 54:245.
- Al-Nadabi HH, Maharachchikumbura SSN, Agrama H, Al-Azri M, Nasehi A, Al-Sadi AM. 2018. Molecular characterization and pathogenicity of *Alternaria* species on wheat and date palms in Oman. *European Journal of Plant Pathology* 152:577–588.
- Barr DJ. 1986. *Allochytridium expandens* rediscovered: morphology, physiology and zoospore ultrastructure. *Mycologia* 78:439–448.
- Bohannon RG, Naeser CW, Schmidt DL, Zimmermann RA. 1989. The timing of uplift, volcanism, and rifting peripheral to the Red Sea: a case for passive rifting. *Journal of Geophysical Research* 94:1683–1701.
- Cubeta MA, Echandi E, Abernethy T, Vilgalys R. 1991. Characterization of anastomosis groups of binucleate *Rhizoctonia* species using restriction analysis of an amplified ribosomal RNA gene. *Molecular Plant Pathology* 81:1395–1400.
- Davis WJ, Letcher PM, Powell MJ. 2013. Chytrid diversity of Tuscaloosa County, Alabama. *Southeast Naturalist* 12:666–683.
- Dayal R. 1997. Chytrids of India. New Delhi, India. 316 p.
- Gouy M, Guindon S, Gascuel O. 2010. SeaView version 4: a multiplatform graphical user interface for sequence alignment and phylogenetic tree building. *Molecular Biology and Evolution* 27:221–224.
- Halo BA, Maharachchikumbura SSN, Al-Yahyai RA, Al-Sadi AM. 2019. *Cladosporium omanense*, a new endophytic species from *Zygophyllum coccineum* in Oman. *Phytotaxa* 388:145–154.
- Karling JS. 1964. Indian chytrids. III. Species of *Rhizophlyctis* isolated on human fibrin film. *Mycopathologia et Mycologia Applicata* 23:215–222.
- Karling JS. 1968. Some zoosporic fungi of New Zealand. III. *Phlyctidium*, *Rhizophyidium*, *Septosperma*, and *Podochytrium*. *Sydowia* 20:74–85.
- Katoh K, Misawa K, Kuma K, Miyata T. 2002. MAFFT: a novel method for rapid multiple sequence alignment based on fast Fourier transformation. *Nucleic Acids Research* 30:3059–3066.
- Katoh K, Rozewicki J, Yamada KD. 2019. MAFFT online service: multiple sequence alignment, interactive sequence choice, and visualization. *Briefings in Bioinformatics* 20:1160–1166.
- Kumar S, Stecher G, Tamura K. 2016. MEGA7: Molecular Evolutionary Genetics Analysis version 7.0 for bigger datasets. *Molecular Biology and Evolution* 33:1870–1874.
- Lanfear R, Calcott B, Ho SYW, Guindon S. 2012. PartitionFinder: combined selection of partitioning schemes and substitution models for phylogenetic analysis. *Molecular Biology and Evolution* 29:1695–1701.
- Lanfear R, Frandsen PB, Wright AM, Senfeld T, Calcott B. 2016. PartitionFinder 2: new methods for selecting partitioned models of evolution for molecular and morphological phylogenetic analyses. *Molecular Biology and Evolution* 34:772–773.
- Larsson A. 2014. AliView: a fast and lightweight alignment viewer and editor for large data sets. *Bioinformatics* 30:3276–3278.
- Leshem T, Letcher PM, Powell MJ, Sukenik A. 2016. Characterization of a new chytrid species parasitic on the dinoflagellate, *Peridinium gatunense*. *Mycologia* 108:731–743.
- Letcher PM, Powell MJ. 2005. *Kappamyces*, a new genus in the Chytridiales (Chytridiomycota). *Nova Hedwigia* 80:115–133.
- Letcher PM, Powell MJ. 2012. A taxonomic summary and revision of *Rhizophyidium* (Rhizophydiales, Chytridiomycota). Tuscaloosa, Alabama: University of Alabama Printing. 216 p.
- Letcher PM, Powell MJ, Churchill PF, and Chambers JG. 2006. Ultrastructural and molecular phylogenetic delineation of a new order, the Rhizophydiales (Chytridiomycota). *Mycological Research* 110:898–915.
- Letcher PM, Vélez CG, Barrantes ME, Powell MJ, Churchill PF, Wakefield WS. 2008. Ultrastructural and molecular analyses of Rhizophydiales (Chytridiomycota) isolates from North America and Argentina. *Mycological Research* 112:759–782.
- Maharachchikumbura SNA, Al-Sadi AM, Al-Khorousi M, Al-Saady N, Hyde KD. 2016. A checklist of fungi in Oman. *Phytotaxa* 273:219–261.
- Mouchacca J. 2005. Mycobiota of the arid Middle East: check-list of novel fungal taxa introduced from 1940 to 2000 and major recent biodiversity titles. *Journal of Arid Environments* 60:359–387.
- Mouchacca J. 2016. Mycological discoveries in the Middle East region in the second part of the last century. *Microbial Biosystems* 1:1–39.
- Moussa TAA, Al-Zahrani HS, Almaghrabi OA, Abdelmoneim TS, Fuller MP. 2017. Comparative metagenomics approaches to characterize the soil fungal communities of western coastal region, Saudi Arabia. *PLoS ONE* 21:e0185096.
- Potato Export Guide. 2019. Agriculture and Rural Economy Directorate. Scottish Government. [cited 2019 Jan 15]. Available from: <https://www.gov.scot/publications/potato-exports-guide/t-to-z/united-arab-emirates/>
- Ronquist F, Teslenko M, Van der Mark P, Ayres DL, Darling A, Höhna S, Larget B, Liu L, Suchard MA, Huelsenbeck JP. 2012. MrBayes 3.2: Efficient Bayesian phylogenetic inference and model choice across a large model space. *Systematic Biology* 61:539–542.
- Stamatakis A. 2006. RAXML-VI-HPC: maximum likelihood-based phylogenetic analysis with thousands of taxa and mixed models. *Bioinformatics* 22:2688–2690.
- Stamatakis A. 2014. RAXML version 8: a tool for phylogenetic analysis and post-analysis for large phylogenies. *Bioinformatics* 30:1312–1313.
- Stamatakis A, Hoover P, Rougemont J. 2008. A rapid algorithm for the RAXML web servers. *Systematic Biology* 57:758–771.
- Tipton L, Zahn G, Datlof E, Kivlin SN, Sheridan P, Amend AS, Hynson NA. 2019. Fungal aerobiotia are not affected by time nor environment over a 13-y time series at the Mana Loa Observatory. *Proceedings of the National Academy of Sciences of the United States of America* 116:25728–25733.
- Van den Wyngaert S, Seto K, Rojas-Jimenez K, Kagami M, Grossart HP. 2017. A new parasitic chytrid, *Staurastromyces*

- oculus* (Rhizophydiales, Staurastromycetaceae fam. nov.), infecting the freshwater desmid *Staurastrum* sp. Protist 168:392–407.
- Vilgalys R, Hester M. 1990. Rapid genetic identification and mapping of enzymatically amplified ribosomal DNA from several *Cryptococcus* species. Journal of Bacteriology 172:4238–4246.
- White TJ, Bruns T, Lee S, Taylor JW. 1990. Amplification and direct sequencing of fungal ribosomal RNA genes for phylogenetics. In: Innis MA, Gelfand DH, Sninsky JJ, White TJ, eds. PCR protocols: a guide to methods and applications. New York: Academic Press. p. 315–322.
- Willoughby LG. 1971. Aquatic fungi from an Antarctic island and a tropical lake. Nova Hedwigia 22:469–488.